



Trends in
**Applied Sciences
Research**

ISSN 1819-3579



Academic
Journals Inc.

www.academicjournals.com

Structural and Morphological Features of Graphitised Carbon Fibres

¹N.S. Babu, ²S.B. Tiwari and ²B. Nageswara Rao

¹Programme Planning and Evaluation Group,

²Structural Analysis and Testing Group,

Vikram Sarabhai Space Centre, Trivandrum - 695022, India

Abstract: Studies are made on graphitised carbon fibres using wide-angle X-ray diffraction technique and Scanning/Transmission Electron Microscopy (SEM/TEM) to obtain structural parameters and morphological features of the fibres. Two important crystallite size structural parameters L_a and L_c can be generally obtained from X-ray diffraction technique. L_c values are evaluated by applying the necessary correction factors for the non-separation of $K\alpha_1$ and $K\alpha_2$ doublet and instrumental broadening. For simplicity empirical expressions are developed for these correction factors from the standard monograms. The surface features of pitch and PAN graphitised carbon fibres at high resolution are examined using SEM and orientation studies are made using TEM. Finally crystallite domain size parameters are related to the tensile modulus of the fibres. It is found that the crystallite domain size increases with the graphitisation temperature and stretching loads. This in turn leads to the enhancement in the tensile modulus of the fibre.

Key words: Carbon fibres, crystallite domain size, tensile modulus, X-ray diffraction technique, SEM, TEM

Introduction

Surface characteristics of materials are related with their crystallinity, especially for carbon materials whose structures range from amorphous stage with high surface activity like activated carbon to high by graphitized carbons. Therefore, it is important to know the change of the crystallinity of the carbon fibres with Heat-treatment-temperature (HTT) in order to understand the change of the surface characteristics of the fibre with HTT. Singh *et al.* (2000) examined the effect of heat treatment on mechanical properties of reinforcing carbon fibres. For a thorough characterization of the graphitized carbon fibers, wide-angle X-ray diffraction technique and Scanning/Transmission Electron Microscopy (SEM/TEM) experiments are essential (Williams and Carter, 1996; Cullity and Stock, 2001; Babu *et al.*, 2003; Sodomka, 2005).

In the contribution it is being proposed, how to determine and measure quantitatively the degree of graphitization of carbon fibres from the X-ray diffractometry technique. The crystallite domain size (L_c) values are evaluated by applying the necessary correction factors for the non-separation of $K\alpha_1$ and $K\alpha_2$ doublet and instrumental broadening. SEM is used to examine the surface morphological features of both low and high modulus carbon fibres, whereas TEM is being used to evaluate preferred orientation of the fibril with respect to the fibre axis. Studies are made to examine the effects of graphitization with respect to temperature and stretching loads.

Corresponding Author: Dr. B. Nageswara Rao, Structural Analysis and Testing Group, Vikram Sarabhai Space Centre, Trivandrum - 695022, India Tel: +91-471-2565831 Fax: +91-471-2564181

Characterization of Carbon Fibres

The X-ray diffraction technique has been primarily used to measure two structural parameters (viz., L_c and L_a) by the analysis of the line shapes of the powdered graphite or fiber samples. These parameters represent the apparent average dimensions of the coherent crystalline domains parallel (L_c) and perpendicular (L_a) to the crystallite c-axis. The word ‘apparent’ has been emphasized because a diffraction line shapes depend on other crystal structure imperfections in addition to the crystallite size.

Evaluation of Crystallite Domain Size

A typical X-ray diffraction pattern of carbon fibres is shown in the Fig. 1. The d_{002} spacing is calculated from the position at the maximum peak height. The maximum position is determined by the mid-point of the peak width at half -height.

The lattice spacing is calculated from the Bragg equation as:

$$n\lambda = 2d \sin\theta \quad (1)$$

Where, $\lambda = 1.5418 \text{ \AA}$, is the wavelength of X-rays, d is the distance between planes of the same Miller indices and θ is the angle of diffraction. The dimensions L_c and L_a of graphite crystallites are generally be calculated from the half-widths of the (002) peak and (100) peak.

The Scherrer equation:

$$L = \frac{K\lambda}{\beta \cos\theta} \quad (2)$$

The relationship (2) between crystallite size and X-ray line broadening derived by Scherrer states that the average crystallite dimension (L) is directly proportional to the wave-length (λ) in angstroms and inversely proportional to the pure diffraction broadening (β) and the cosine of the Bragg angle (θ). The constant K depends largely upon the crystallite shape, the (hkl) indices and the definitions taken for β and L . Values from 0.7 to 1.70 have been assumed for K by different investigators; many researchers arbitrarily set it equal to 1.0 for the sake of uniformity in published results. Since in most cases the crystallite shape is unknown and may vary from crystal to crystal, it is probably best to define L as the mean dimension of the crystallite perpendicular to the diffracting planes (d_{hkl}). This definition has been shown to give a K value of about 0.9 when β is taken as the half-maximum line breadth. Apparent stacking height (L_c) and apparent layer size (L_a) were calculated using the Scherrer Eq. (2) in which the constant $K = 0.9$ for calculation of L_c and $K = 0.9 + (1.84 - 0.9)p$, for calculation of L_a , p being the proportion of disoriented layers in the graphite as derived from the expression (Hawthorne, 1971): $d_{002} = 3.440 - 0.086(1 - p^2)$. Input data required for the determination of the pure diffraction breadth (β) are the observed half-maximum breadth (B_0), the diffraction angle (2θ) at which the peak occurs, the instrumental broadening (b) at this angle and the angular separation (Δ).

Correction of Measured Line Breadth

Direct measurement of the half maximum line breadth B_0 can be made on diffraction peaks, which are recorded at slow goniometer speeds and fast chart speeds. This combination will generally permit the most precise determination of B_0 . The time constant and recorder range should be set to produce a smooth background and nearly full-scale intensity. The half-maximum line breadth B_0 must be corrected for $K\alpha$ -doublet separation if unresolved radiation is being used. The angular separation for $\text{Cu } K\alpha$ radiation:

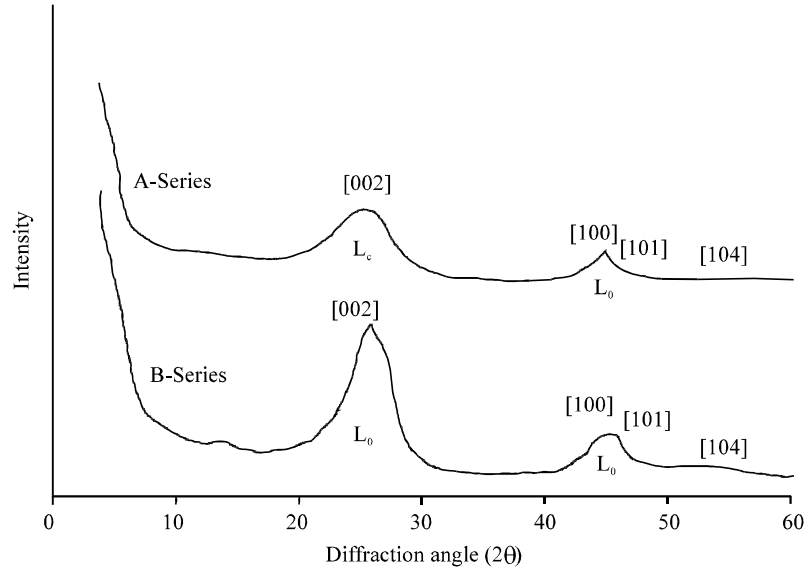


Fig. 1: A typical X-ray diffraction pattern of carbon fibres

$$\Delta = 0.285 \tan\theta \quad (3)$$

Barton (1967) has presented a “ B/B_0 versus Δ/B_0 ” curve for correcting line breadths for $K\alpha$ -doublet broadening. From the observed half-maximum breadth (B_0) and the diffraction angle (2θ) at which the peak occurs, the ratio of Δ/B_0 is calculated using Eq. 3 to obtain the corrected breadth (B) from the correction curve.

Choice of a suitable standard is most important to the determination of crystallite size. Ideally a powdered strain-free sample of the same material as the unknown should be used. It should consist only of crystallites in the range from 10,000 to 100,000 Å. If such a sample is not available, the reference standard should lie in this crystallite-size range have similar X-ray absorbtivity and produce peaks near those in the unknown. For a given set of instrumental conditions, the half-maximum peak breadth b_0 (corrected for $K\alpha$ doublet broadening) thus obtained can be taken as true instrumental broadening (b). The half-maximum line breadths of the diffraction peaks of the reference standard may then be plotted as a function of diffraction angle (2θ). Such a graph presented by Barton (1967) is used in the present study to determine the instrumental broadening b for the diffraction angle. With the corrected peak breadth (B) and the instrumental broadening (b), determined, the pure diffraction breadth (β) is found from the curves of Barton (1967).

Empirical Relations for Pure Diffraction Breadth

All the curves of Barton (1967) are represented by the following empirical relations for pure diffraction breadth:

$$\frac{B}{B_0} = f_1\left(\frac{\Delta}{B_0}\right) \quad (4)$$

$$b = 0.2813 - f_2(\theta), \quad (5)$$

$$\frac{\beta}{B} = f_3 \left(\frac{b}{B} \right) \quad \text{for } \theta \leq 90^\circ$$

$$= 1 - \frac{b}{B} \quad \text{for } \theta \geq 90^\circ$$
(6)

Where

$$f_1(x) = \left(\frac{9197}{6500} - \frac{17}{13}x \right) \left[1 + \left\{ \frac{1623}{1175} - \frac{60}{47}x \right\}^{\frac{1157}{200}} \right]^{\frac{200}{1157}}$$
(7)

$$f_2(x) = \left(\frac{180 - 2x}{940} \right) \left\{ 1 + \left(\frac{180 - 2x}{130} \right)^{\frac{9}{2}} \right\}^{-\frac{2}{9}}$$
(8)

$$f_3(x) = \frac{3461}{3000}(1-x) \left[1 + \left\{ \frac{3461}{3000}(1-x) \right\}^{\frac{123}{5}} \right]^{\frac{5}{123}}$$
(9)

Impact of Correction Factors on L_c Measurements

Earlier studies on carbon fibres using wide-angle X-ray diffraction technique were not accounted the essential correction factors while evaluating the crystallite domain size, L_c . A comparative study is made considering the published test data to demonstrate the impact of correction factors on L_c measurements.

A simple computer program is written utilizing the Eq. (1) to (9) for the accurate evaluation of the crystallite-size. Hawthorne (1971) has presented some of the mechanical and physical properties of strain graphitised glassy carbon fibres and correlated them with their crystallographic parameters and heat-treatment temperatures. Table 1a gives the comparison of L_c values with and without correcting X-ray diffractometer line breadths for petroleum pitch-based carbon fibres strain graphitised to various extents at the heat-treatment temperature of 2850°C. It can be seen from the results presented in Table 1 that the pure diffraction breadth (β) values are lower than those of the half-maximum line breadth (B_0), which are directly measured from diffraction peaks. Hawthorne (1971) used B_0 values for β in Eq. (2) while evaluating the structural parameter (L_c). The discrepancy in L_c values of Hawthorne (1971) and those of present analysis is mainly due to the lower values of β . Table 1b gives L_c values of the present analysis for petroleum pitch-based carbon fibres heat-treated to various temperatures from the measured values (Hawthorne, 1971) of B_0 and θ . The structural parameter (L_c) increases with the heat-treatment temperature. Test results presented by Hawthorne (1971) for hot-stretched petroleum-pitch-based fibres indicate the enhancement of graphitisation with consequently lower values of d-spacing for fibres heat-treated under stress. The “turbostratic value is only reached at heat-treatment temperatures well above 2000°C and no fibre approaches the true graphitic value.

Table 2 gives L_c values of the present analysis for GSCY2.5 carbon filament wound/CVD carbon infiltrated cylinders from the measured values (Leeds, 1973) of B_0 and θ . Wicks (1975), as well as Wicks and Coyle (1976) have examined micro-structural inhomogeneity in carbon fibres. Table 3 gives L_c values of the present analysis for different types of carbon fibres from the measured values (Wicks, 1975) of B_0 and θ .

Table 1a: Structural parameter (L_c) for the strain graphitized glassy carbon fibres heat-treated at 2850°C

Percentage elongation	Hawthorne (1971)				Present analysis			
	d_{002} (Å)	L_c (Å)	2θ (degrees)	B_0 (degrees)	B (degrees)	b (degrees)	β (degrees)	L_c (Å)
0	3.41	33.0	26.132	2.473	2.401	0.091	2.394	34.096
20	3.42	28.5	26.054	2.863	2.781	0.091	2.774	29.421
40	3.42	44.0	26.054	1.855	1.798	0.091	1.791	45.571
60	3.42	47.5	26.054	1.718	1.665	0.091	1.657	49.239
80	3.42	51.0	26.054	1.600	1.550	0.091	1.542	52.915
100	3.42	60.0	26.054	1.360	1.316	0.091	1.307	62.417
120	3.40	89.0	26.210	0.917	0.884	0.091	0.871	93.730
160	3.41	116.0	26.132	0.704	0.675	0.091	0.656	124.51
180	3.41	145.0	26.132	0.563	0.537	0.091	0.508	160.57

Table 1b: Structural parameter (L_c) for the petroleum pitch-based carbon fibres heat-treated to various temperatures

HTT (°C)	Hawthorne (1971)				Present analysis			
	d_{002} (Å)	L_c (Å)	2θ (degrees)	B_0 (degrees)	B (degrees)	b (degrees)	β (degrees)	L_c (Å)
1000	3.72	11.0	23.920	7.388	7.190	0.091	7.179	11.321
1500	3.58	15.2	24.870	5.356	5.210	0.091	5.201	15.654
2000	3.47	25.2	25.672	3.236	3.144	0.091	3.137	25.997
2500	3.46	26.9	25.747	3.032	2.945	0.091	2.938	27.760
2750	3.44	32.0	25.900	2.549	2.475	0.091	2.468	33.055
2850	3.41	33.3	26.132	2.451	2.379	0.091	2.372	34.408

Table 2: Values of structural parameter (L_c) for GSC Y25 carbon filament wound/CVD carbon composites

HTT (°C)	Leeds (1975)				Present analysis			
	d_{002} (Å)	L_c (Å)	2θ (degrees)	B_0 (degrees)	B (degrees)	b (degrees)	β (degrees)	L_c (Å)
3000	3.42	57.5	26.054	1.422	1.377	0.091	1.368	59.773
2750	3.43	55.0	25.977	1.496	1.449	0.091	1.440	57.140
2500	3.45	50.0	25.862	1.648	1.597	0.091	1.589	51.872
2000	3.45	43.194	25.823	1.926	1.868	0.091	1.861	43.308

Table 3: Values of structural parameter (L_c) for different types of carbon fibres

Neutron dose (nvt)	Hawthorne (1971)				Present analysis			
	d_{002} (Å)	L_c (Å)	2θ (degrees)	B_0 (degrees)	B (degrees)	b (degrees)	β (degrees)	L_c (Å)
High tensile strength PAN carbon fibre heat-treated at 1600°C								
Unirradiated	3.49	21.0	25.522	3.968	3.858	0.091	3.850	21.176
1.0E+17	3.49	19.0	25.522	4.386	4.265	0.091	4.256	19.153
1.5E+19	3.64	16.0	24.454	5.197	5.056	0.091	5.046	16.120
7.0E+19	3.74	14.0	23.790	5.933	5.772	0.091	5.762	14.100
High-modulus PAN carbon fibre heat-treated at 2500°C								
Unirradiated	3.40	68.0	26.210	1.227	1.186	0.091	1.177	69.358
1.0E+17	3.41	64.0	26.132	1.304	1.261	0.091	1.252	65.188
1.5E+19	3.43	52.0	25.977	1.604	1.554	0.091	1.546	52.777
7.0E+19	3.54	41.0	25.156	2.301	1.970	0.091	1.963	41.497
PAN 70 carbon fibre heat-treated at 3000° C								
unirradiated	3.41	65.0	26.132	1.284	1.241	0.091	1.232	66.228
1.0E+17	3.43	64.0	25.977	1.303	1.261	0.091	1.252	65.185
1.5E+19	3.46	55.0	25.747	1.516	1.468	0.091	1.460	55.864
7.0E+19	3.53	35.0	25.228	2.379	2.310	0.091	2.303	35.381

X-ray Diffraction Analysis

Using metallographic techniques, the characterization of pure graphite, high-modulus PAN fiber of Torayca of Japan, high-modulus Pitch fiber of Union Carbide Company of USA and low-modulus PAN fiber of Sigril of UK are highlighted in this research.

Philips X-ray diffraction unit with PW 1729 X-ray generator with vertical goniometer using PW1710 computer controlled diffractometer was used to carry out the X-ray diffraction analysis on pure graphite and other high and low modulus fibers.

The Co $k\alpha$ radiation was used with an accelerating voltage of 35 kV and a tube current of 20 mA. Iron filter was used to filter the $k\beta$ radiation. Proportional counter tuned at 1700 volts was used as the detector. The diffractograms were recorded at a slower speed of 10 mm/min. The receiving slit of 0.5° and incident beam slit of 1.0° was used. Sample spinner was used to rotate the sample to avoid possible preferred orientation in the sample. Sample preparation was carried out by mounting the fibers on nylon holder by means of adhesive tape that will not give reflections of its own. For measuring the crystallite size L_c in the direction perpendicular fiber axis, recorder full-scale of 2000 was used. But to record the spectrum of (100) and (101) peaks having lower intensity, highly sensitive recorder full-scale of 200 was used. A scale of RFS 100 less than RFS 200 did not yield meaningful spectrum delineating the crystalline peaks of (100) and (101) from the background noise. To get a smooth Spectrum Recorder Time Constant (RTC) of 5 was used. Scan range of 2θ (Bragg angle) was selected from 24° to 36° to record a spectrum of (002) peaks. To record (100) and (101) peaks, a scan range of 2θ from 45° to 55° was selected and to measure the crystallite size (a-direction) in the breadth direction right hand shoulder in the lower angle side was used. However to record a continuous spectrum of pure graphite, a scan range of 2θ from 28° to 54° was used with a recorder full-scale of 500 pulses for the full scale.

Scanning Electron Microscopy (SEM) Analysis

This tool is useful for surface evaluation along the axis of carbon fibers as well as in their cross-sections and also useful to measure fiber diameter. Cambridge Stereo-scan 250Mk SEM was used to examine the surface morphology of the fibers. The carbon fibers were fixed on the holder using silver paint with the fiber axis parallel to the electron beam. The irregularities of the fibrous surface were examined in detail under high magnification in low modulus fibers as shown in the Fig. 2. The cross-sectional morphology of the high-modulus fibers revealed the radial orientation of basal planes (Fig. 3).

Transmission Electron Microscopy (TEM) Analysis

A Hitachi H 8000, 200 kV Transmission Electron Microscope (TEM) was employed for the characterization of the high modulus fibers. The fibers were ground to 600# size and suspended in water. Better suspension was ensured by ultrasonic vibration at 400 kHz. These suspensions were placed on the carbon film deposited on a Cu grid of 3mm diameter.

The Selected Area Diffraction (SAD) pattern of high modulus PAN fiber was shown in the Fig. 4a and the corresponding structure in Fig. 4b. As the thickness of the fiber was more than 1000\AA at the centre, the structure was revealed only at the edges. The SAD pattern revealed (002) and (100) reflections and the image of the interior substructure of the fibers.

Results and Discussion

The crystallite domain size perpendicular to the fibre axis (L_c) for graphitized PAN carbon fibre at different heat-treatment-temperatures (HTT) is measured. From the recorded X-ray diffractograms,

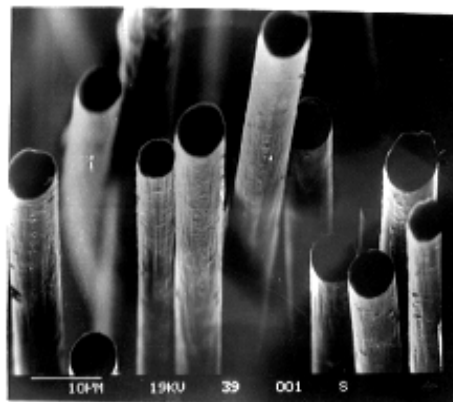


Fig. 2a: Bundle of low modulus fibres

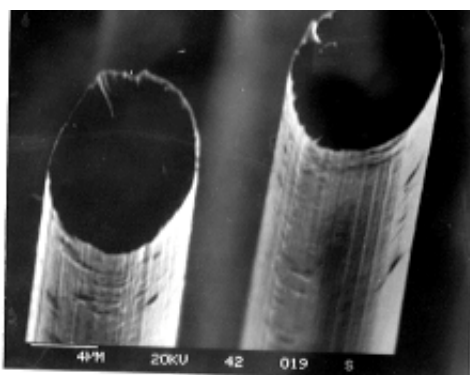


Fig. 2b: Low modulus fibres depicting the striations on the surface

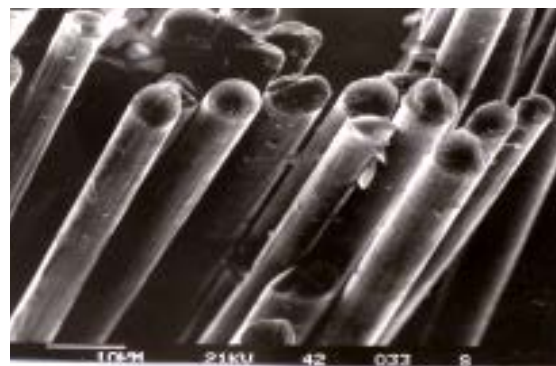


Fig. 3a: Bundle of high modulus fibres heat-treated at 2500°C



Fig. 3b: High modulus fibres depicting radial alignment

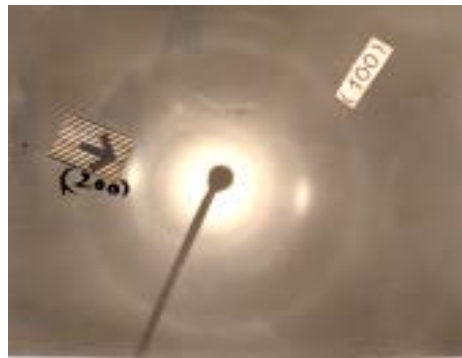


Fig. 4a: Selected area diffraction pattern of high-modulus PAN fibre from TEM



Fig. 4b: Structure of the high-modulus PAN fibre from TEM

Table 4: Values of structural parameter (L_c) for graphitized PAN carbon fibre at different heat-treated temperatures

HTT (°C)	2θ (degrees)	B_0 (degrees)	B (degrees)	b (degrees)	β (degrees)	L_c (Å)
2275	30.5	2.5	2.425	0.093	2.418	34.079
2500	30.3	2.4	2.328	0.092	2.321	35.492
2900	30.0	2.1	2.036	0.092	2.028	40.579

Table 5: Values of structural parameter (L_c) for graphitized PAN carbon fibre heat-treated at 2275°C at different stretching loads

Stretching load (grams)	2θ (degrees)	B_0 (degrees)	B (degrees)	b (degrees)	β (degrees)	L_c (Å)
0	30.5	2.5	2.425	0.093	2.418	34.079
50	30.1	2.4	2.328	0.092	2.321	35.474
200	30.0	2.2	2.133	0.092	2.126	38.718

Table 6: Values of structural parameter (L_c) for graphitized carbon fibres having variation in Young's modulus

Young's modulus (Gpa)	2θ (degrees)	B_0 (degrees)	B (degrees)	b (degrees)	β (degrees)	L_c (Å)
520 ^a	30.0	0.8	0.767	0.092	0.751	109.597
490 ^b	32.0	0.9	0.864	0.093	0.850	97.278
235 ^c	29.0	4.7	4.570	0.092	4.561	18.006

^a Pitch fiber of Union carbide company of USA, ^b PAN fibre of Torayca of Japan, ^c PAN fibre of Sigril of UK

full width at half maximum (B_0) and Bragg angle (2θ) at different temperatures are noted and presented in Table 4. L_c value is evaluated with the corrected peak breadth (B), the instrumental broadening (b) and the pure diffraction breadth (β). It can be seen from the results in Table 4 that L_c increases with the HTT of the PAN carbon fibre.

An attempt is made to understand the effect of stretching load on the structural parameter (L_c) for the PAN carbon fibre heated at 2275°C. It can be seen from the results in Table 5 that L_c increases with increasing the stretching load.

Finally, to examine the effect of L_c values on Young's modulus, the X-ray diffraction patterns are obtained for high modulus Pitch fiber of Union Carbide Company of USA with 520 GPa modulus, high-modulus PAN fiber of Torayca of Japan with 490 GPa modulus and high strength low modulus Sigril PAN fiber with 235 G Pa. The details of measurements made in this study are presented in Table 6. It is noted that L_c increases with increasing in Young's modulus. At a constant heat-treatment temperature, the pitch-based carbon fibres are found to be more graphitizable and give a larger stacking height than the PAN based carbon fibres as observed by Takaku and Shioya (1990). It is noted from the investigations of Ko and Huang (1992) that the PAN fibres modified with Cobaltous chloride have a greater crystal size, a higher crystallinity and a better molecular orientation than the original PAN fibres.

Conclusions

In the new textile composite technology the carbon fibres are being frequently used. Their properties are being determined through their structure. Wide-angle X-ray diffraction technique is used to obtain the structural parameter (L_c) for PAN and pitch-based carbon fibres. The irregularities of the fiber surface and its cross-sectional features are examined using SEM. The internal features like orientation of layers along the fiber axis are also examined using TEM.

It is noted from the present analysis that values of crystallite size (L_c), using the pure diffraction breadth (β) are found to be higher than those obtained from the directly measured half-maximum line breadth (B_0). There is no significant affect on the measured interlayer spacing (d_{002}), which is evident from the measured Bragg angle values at the higher temperatures. Higher temperature treatment for

graphitisation has increased L_c values and the same steep in values of L_c is found with stretching loads even lower graphitisation temperature. It is also observed that values of L_c are increased with increase in the Young's modulus.

Scanning electron micrographs have clearly revealed the smooth surface structure of high modulus fibers and striations on the surface in the case of low modulus fibers and striations on the surface in the case of low modulus fibers. Selected area diffraction has confirmed the preferred orientation of (002) basal planes in the fiber axis direction. TEM micrograph indicates parallel basal planes at the edges at higher magnification.

Acknowledgements

The authors would like to thank the reviewers of the VSSC Editorial Board for their valuable suggestions to improve the clarity of this article. They wish to thank Mr. K. Naveena Kumar (Head, PPEG) and Mrs. T.S. Rama Devi (Deputy Director, VSSC) for encouragements and Dr. B.N. Suresh (Director, VSSC) for giving permission to publish this article.

References

- Babu, N.S., B.N. Rao, S. Suresh Kumar, R. Venkateswaran and K. Sree Kumar, 2003. Structural parameters and morphological features of pitch and polyacrylonitrile graphitised carbon fibres. Proceedings of the National Seminar on Non-Destructive Evaluation, Organized by ISNDT, Trivandrum, India, pp: 258-263.
- Barton, S.F., 1967. Crystallite-size Determination from Line Broadening and Spotty Patterns. In The Handbook of X-rays for Diffraction, Emission, Absorption and Microscopy, (Kaelble, E.F. Ed.), McGraw-Hill Book Company York.
- Cullity, B.D. and S.R. Stock, 2001. Elements of X-ray Diffraction, Prentice Hall, NJ.
- Hawthorne, H.M., 1971. Structure and properties of strain graphitized glassy carbon fibres. International Conference on Carbon Fibres, The Plastics Institute of London.
- Ko, T.H. and L.C. Huang, 1992. Preparation of high performance carbon fibres. J. Mater. Sci., 27: 2429-2436.
- Leeds, D.H., 1973. The relationship between thermal history, X-ray crystallographic structure and thermal properties of rayon precursor carbon-carbon composites-A literature review. Proceedings of the 18th National Symposium and Exhibition on New Horizons in Materials and Processing, Los Angeles.
- Singh, I., O.P. Bahl and S.K. Barthwal, 2000. Effect of Heat Treatment of Reinforcing Carbon Fibres on Mechanical Properties of Composites. In 'High Temperature Fibre Composite Materials' (Srivastava, V.K. Ed.), Allied Publ. Ltd., New Delhi, India, pp: 87-91.
- Sodomka, L., 2005. Degree of graphitization of carbon fibres. Materials Structures, 12: 93-95.
- Takaku, A. and M. Shiyoa, 1990. X-ray measurements and the structure of polyacrylonitrile and pitch-based carbon fibres. J. Mater. Sci., 25: 4873-4879.
- Wicks, B.J., 1975. Microstructural disorder and the mechanical properties of carbon fibres. J. Nuclear Materials, 56: 287-296.
- Wicks, B.J. and R.A. Coyle, 1976. Microstructural inhomogeneity in carbon fibres. J. Mater. Sci., 11: 376-386.
- Williams, D.B. and C.B. Carter, 1996. Transmission Electron Microscopy. Plenum Press, New York.